Supporting information for:

Electronic Coupling between Ligand and Core Energy States in Dithiolate-Monothiolate Stabilized Au Clusters

Tarushee Ahuja,[§] Dengchao Wang, [§] Zhenghua Tang,[¥] Donald Robinson, Jonathan Padelford and Gangli Wang*

Department of Chemistry, Georgia State University, Atlanta, Georgia 30302

[§]:These authors contributed equally;

[¥]: New Energy Research Institute, School of Environment and Energy, South China University of Technology, Guangzhou Higher Education Mega Center, Guangzhou, China, 510006.

[†]:Department of Chemistry, The University of Texas at Austin, 105 East 24th Street Stop A5300, Austin, Texas 78712-1224, United States.

Figure SI-1. The UV-vis absorption spectrum of the Au_{130} nanoclusters.

Figure SI-2. MALDI mass spectra of Au_{130} nanoclusters.

Figure SI-3. Cylic voltamgram of Durene-DT ligand at 10 mM concentration in CH_2Cl_2.

Normal Pulse Voltammetry

Estimation of the lifetime of the intermediate (+0.9 V).

Figure SI-4. Chronoampermetry analysis of the Au_{130} nanoclusters with ligand oxidation (+1.6 V) and three reversal reduction process (-0.5, 0 and 0.7 V) at different time scale.

Figure SI-5. Peak current analysis of the reversal reduction peaks at +0.9 and -0.5 V in CV at different scan rates (Data are from Figure 2).

Figure SI-6. A: Absorption spectrum, B: cyclic voltammograms and C: the charge analysis of plasmonic Au-Durene-DT nanoparticles.

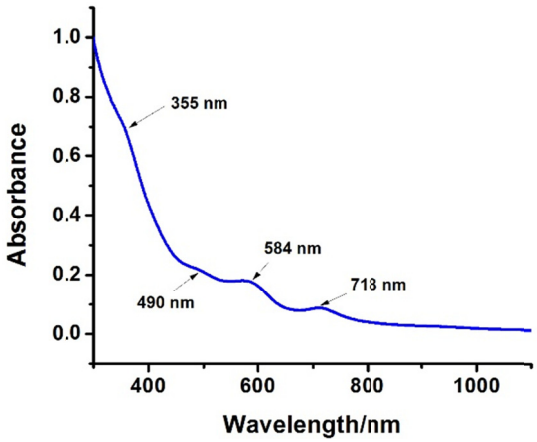

Figure SI-1. UV-vis absorption spectrum of Au_{130} nanoclusters in CH_2Cl_2. Four discrete bands at 355 nm, 490 nm, 584nm and 718nm are characteristis of the Au_{130} nanoclusters as described in our earlier report.

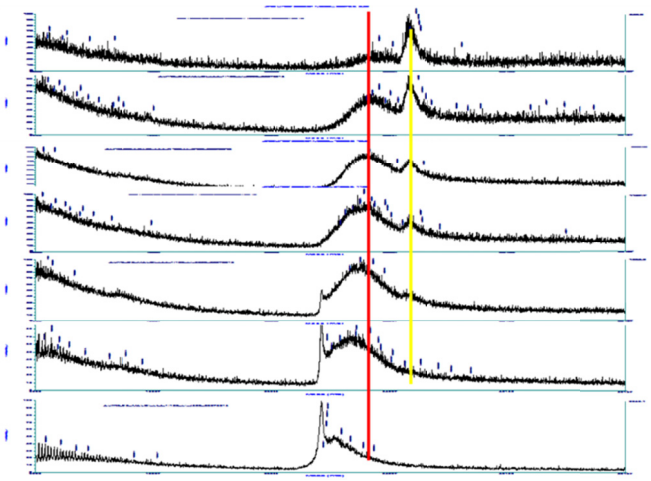

Figure SI-2: The MALDI mass spectra of Au_{130} nanoclusters using DCTB as matrix in linear positive mode. The Au_{130} sample was dissoved in CH_2Cl_2 and dropcasted by sandwich method in 1:100 (Au-MTC:Matrix) ratio. $Au_{130}(Durene\text{-}DT)_{29}(PET)_{22}$ molecular ion at 35313 m/z (aligned with yellow line) was observed at lower laser intensity. The peak intensity decreased and disappeared due to fragmentation when the laser intensity was increased from top to bottom spectra. Meanwhile, peaks at lower m/z ranges, such as thebroad peak around 32K (red line) developed and further shifted to 29.4K. Au-S fragments at lower mass range was observed at higher intensities in linear negative mode. The m/z patterns are consistent with the earlier reports of Au_{130} nanoclusters.

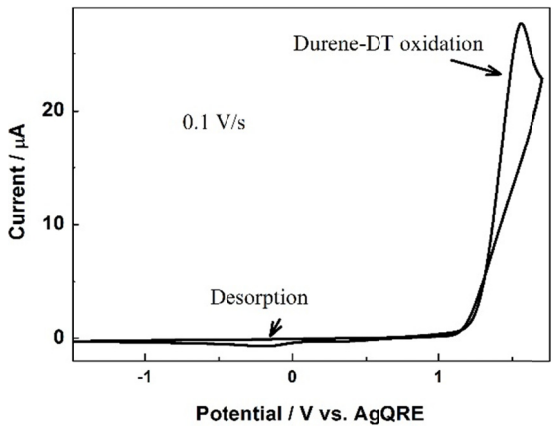

Figure SI-3. Cyclic voltammogram of durene-dithiol at 10 mM concentration. The scan rate is 0.1 V/s in CH_2Cl_2 with 0.1 M TBAP. A large irreversible oxidation peak at 1.5 V corresponds to the oxidation of the Durene-dithiol.

Normal Pulse Voltammetry (NPV)

In NPV, the applied potential is stepped from an unchanged initial potential to sequentially-changed final potentials. The current difference under the two potentials at specific time scale is recorded as one data point at the stepped potential. The technique therefore allows us to maintain consistent initial conditions at the electrode surface to capture different decay or relaxation processes at a certain potential.

Estimation of the lifetime of the intermediate (+0.9 V).

From Figure 2A, the +0.9 V peak becomes distinguishable at a scan rate of 0.4 V/s. As the intermediate is produced immediately after the oxidation of the ligands at +1.34 V(facile ET process), and characterized by the reversal reduction peak at +0.9 V. The lifetime of the intermediate then would be equal to time duration between the two potentials. Noting the upper scan limit is 1.6 V for both forward and backward scans, at the scan rate of 0.4 V/s, the duration time is then can be estimated as:

$t = \Delta V_2/v = (1.6\ V - 0.9\ V)/\ 0.4\ V/s = 1.75\ s.$

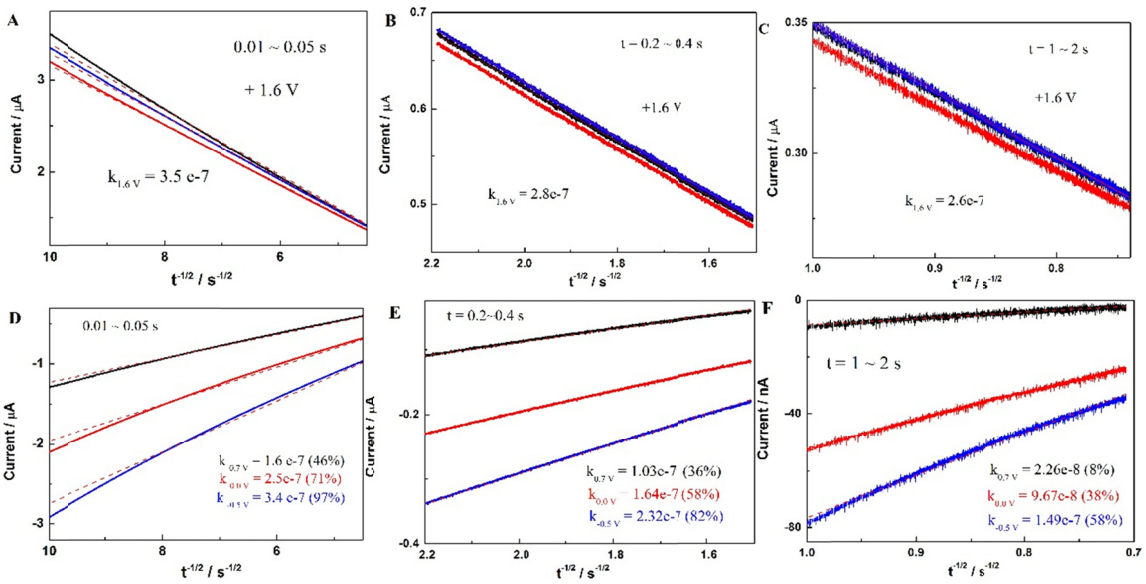

Figure SI-4. Chronoampermetry analysis of the ligand oxidation (+1.6 V) and three reversal reduction processes (-0.5, 0 and 0.7 V) at different time scales. The i- $t^{-1/2}$ curves for ligand oxidation at +1.6 V at short and long time duration are shown in panel A(0.01 to 0.05 s) B (0.2 to 0.4 s) and C(1 to 2 s), while i- $t^{-1/2}$ curves for the three reversal reduction process are shown in panel D(0.01 to 0.05 s) E (0.2 to 0.4 s) and F (1 to 2 s). Solid lines are from experiments and the dash lines from fitting. The slopes of those linear curves at the representative time periods are listed. From the ratio of the reduction curve slopes with respect to the oxidation ones, the percentage of electron transfer numbers at each potential, or energy states, are obtained.

From Panel A and D: 46%; 71%-46%=25%; 97%-71%=26%.

From Panel B and E: 36%; 58%-36%=22%; 82%-58%=24%.

From Panel C and F: 8%; 38%-8%=30%; 58%-38%=20%.

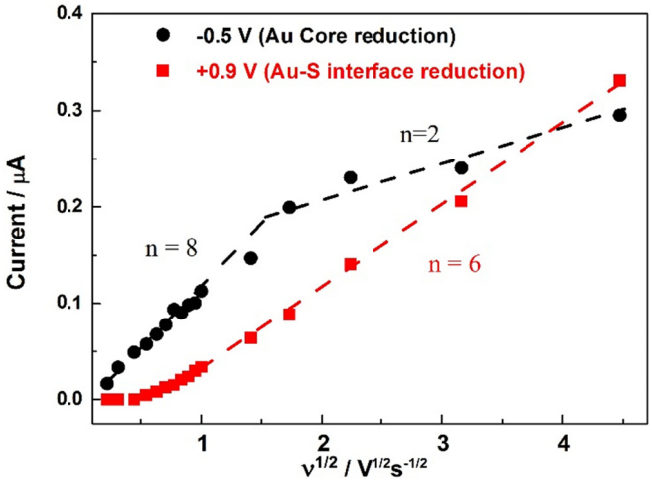

Figure SI-5. Peak current analysis of the reversal reduction peaks at +0.9 and -0.5 V in CVs at different scan rates (Data are from Figure 2, from 0.1 to 20 V/s). Different linear regions at low and high scan rate ranges for the -0.5 and +0.9 V peaks are displayed, indicating different relaxation time scales.

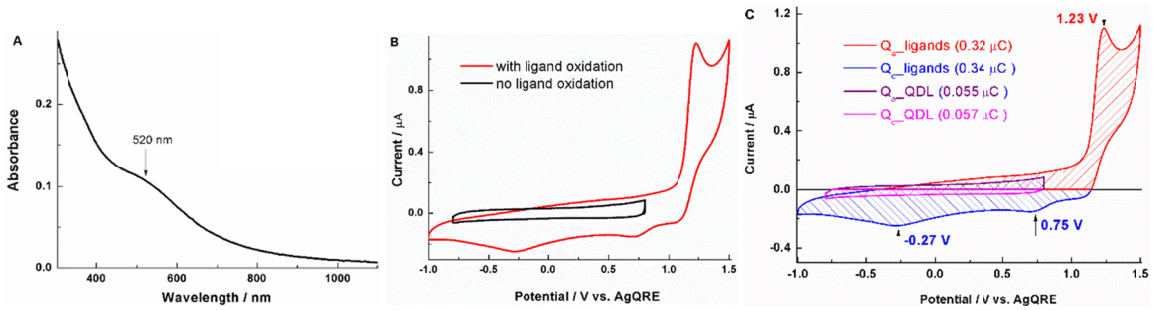

Figure SI-6. A: Absorption spectrum, B: cyclic voltammograms and C: the charge analysis of plasmonic Au-Durene-DT nanoparticles.

The 520 nm band in the absorption spectrum corresponds to the plasmonic bands from a 3.0 nm Au nanoparticles (Whetten and coworkers. J. Phys. Chem. B 1997, 101, 3706-3712). At smaller potential window, ligands are not oxidized (black curve in panel B). The symmetric forward and backward curves include current from both the QDL core charging/discharging and capacitive double layer charging at electrode surface. It is worth reminding that single electron transfer events can not be resolved from plasmonic nanoparticles due to their large core size (thus small charging energy based on concentric sphere model). At a large potential window, once the ligands are oxidized at +1.23 V, new reduction bands at about +0.75 V and -0.27 V are observed in the reversal potential scan. The reduction curve is no longer symmetric to the oxidation one once ligands are oxidized. For the Au_{130} nanoclusters at the same scan rate of 1.0 V/s, the ligand oxidation peak is at +1.34 V, with one reversal reduction peak at +0.86 V, and the other reduction current reach to a plateau around -0.52 V. Note single electron QDL could be resolved from the Au_{130} nanoclusters. In the large Au nanoparticles, those potentials were shifted to less positive (+1.23 V for ligand oxidation and reversal reduction at +0.75 V and -0.27 V) reflecting the impacts by the energy states of the larger metal core. Further, the anodic and cathodic charges integrated from the current-potential loops are comparable for both core ET (symmetric) and new ET features (ligand-induced), suggesting qualitatively similar relaxation processes resulted from the coupling between the core and ligand electrons/energy states.